COVID-19 lockdown a window of opportunity to understand the role of human activity on forest fire incidences in the Western Himalaya, India

Amitesh Gupta, C. M. Bhatt, Arijit Roy* and Prakash Chauhan

Indian Institute of Remote Sensing,
Indian Space Research Organisation, 4, Kalidas Road,
Dehradun 248 001, India

The global COVID-19 pandemic has resulted in a complete lockdown of economic activities and movement across the world. This provides an opportunity to evaluate the impact of minimal anthropogenic activities on forest fire occurrences in the Western Himalaya, India. Significant reduction of 83.4% in the cumulative fire incidences during 24 March to 5 May 2020 was observed in this region compared to the average of fire incidences during the corresponding period of 2006–20. Though during the current lockdown period, precipitation was high (~281 mm) compared to the average for the last 15 years (~125 mm), it did not contribute to the build-up of soil moisture. Comparatively higher NDVI (by 30.59%) and EVI (by 12.18%) in the lockdown phase unlike the average of previous years which showed declining trend, indicates that the lockdown provided an opportunity for the canopy to sustain and have higher vigour; this was not visible earlier due to fire incidences. The present study emphasizes that anthropogenic activities play a major role in forest fire incidences in this region.

Keywords: Coronavirus-19, forest fire, human activity, lockdown, remote sensing.

HUMANS have influenced the environment to such an extent that the halt in anthropogenic activities (across the world) due to the COVID-19 related lockdown has resulted in a sudden relief for different ecosystems across the world[1–3]. Studies across the globe on various aspects of the environment have shown that the new norm has been changed in various areas of the ecosystem functioning. Forest fires in India, which are predominantly of anthropogenic origin are expected to significantly reduce both in extent as well as severity due to the cessation of the anthropogenic activity enforced across the country to contain the spread of COVID-19 (ref. 4). The Government of India had enforced a lockdown across the country from 24 March 2020, which resulted in complete cessation of all economic activities and human movement across the country. The present situation provides a unique opportunity to assess the extent of anthropogenic activities in forest fire initiation and spread in the Western Himalayan states of Uttarakhand and Himachal Pradesh, India which are among the worst affected due to such fires in recent years.

Fire season in the Western Himalayan region starts from March onwards till the middle of June. April and May experience significant number of forest fires in this region. This is due to the accumulation of fuel load as well as conducive environmental and weather conditions for the initiation of forest fires[5,6]. Since the last two decades, space-borne sensor Moderate Resolution Imaging Spectroradiometer (MODIS) on-board TERRA and AQUA satellites has operationally provided active fire locations four times daily, and has been extensively used for fire monitoring along with burnt area assessment[7–11]. Since forest fires have an impact on vegetation conditions, the vegetation indices such as normalized difference vegetation index (NDVI) and enhanced vegetation index (EVI) are essential tools to assess the impact of forest fires[12,13]. On the other hand, land surface temperature (LST) is one of the critical biophysical and/or climatic variables that plays an important role in understanding various environmental phenomena, including forest fire vulnerability[14]. From MODIS observations, the EVI, NDVI, LST products are generated at regular intervals, which help oversee the vegetation health and fire conditions continuously over a larger region. The amount of precipitation also has a significant impact on the occurrence and severity of forest fires[15]. Several researchers have found significant negative association between precipitation and forest fire occurrence[16,17]. Similarly, soil moisture determines the final fire conditions, as dead fuel moisture content is dependent on the preceding weather conditions[18,19], signifying that negative soil moisture anomaly could provide suitable conditions for forest fires.

Most of the research carried out on forest fires in the Indian context and especially in the Himalayan region indicates that majority of fires are due to anthropogenic factors[20,21]. The Western Himalayan region, particularly between elevation zone of 800 and 2000 m, dominated by Chir-pine (*Pinus roxburghii*) associated frequently with Banj oak (*Quercus leucotrichophora*), is exposed to frequent man-made fires[22,23]. Among the major causes of forest fires in the Western Himalayan region are collection of fuelwood, grazing of cattle, burning of pine litter, tourists, hikers, vehicular movement, etc. Due to the lockdown, there has been no movement of vehicles and tourists in the hills of Uttarakhand and Himachal Pradesh. However, activities such as fuelwood collection and grazing around the villages might have taken place in the far-flung areas. A spatio-temporal analysis has provided an important input to identify the agents of forest fire occurrences in the region.

The present study assesses the spatio-temporal patterns of active fire counts, NDVI, EVI, LST and precipitation

*For correspondence. (e-mail: arijitroy@iirs.gov.in)

during the lockdown period (24 March to 5 May 2020) compared with the long-term average observations made during the last 15 years (2006–20) for the same duration. The objective of the study was primarily to understand the impact of lockdown imposed due to the global COVID-19 pandemic on the occurrence of forest fires, and the anthropogenic origin hypothesis of forest fires in the two Himalayan states of Uttarakhand and Himachal Pradesh.

The study areas selected for observation and analysis, i.e. Uttarakhand and Himachal Pradesh, are located in the Indian Himalayan region between 75°35′38.629″–81°2′32.299″E and 28°42′33.171″–33°15′17.298″N. These two states combined cover an area of 109,156 sq. km, which is around 26% of the total geographic area of the Indian Himalayan states. The study area is mostly mountainous and mainly consists of forests, agricultural land, scrubland, grassland, wasteland and ice/snow. The rivers in the study area are perennial and nurtured by melting snow from the mountains and monsoon rainfall, and protected by an extensive cover of natural vegetation. The Greater Himalaya range constitutes most of the northern part of the region, which is covered by high Himalayan peaks and glaciers, whereas agriculture areas largely form the lower foothills. The major vegetation types found in this region are Himalayan moist temperate forests, Himalayan dry temperate forests, subtropical pine forests, subtropical broad-leaved hill forests, tropical deciduous forests, subalpine forests and alpine vegetation[24].

Active fire points located by MODIS observation were downloaded from the Fire Information for Resource Management System (FIRMS) website (https://firms.modaps.eosdis.nasa.gov). These point locations of 1 km spatial resolution are generated within 3 h of satellite overpass under relatively cloud-free conditions using a contextual algorithm[25,26]. Only high-confidence fire points (confidence interval >80%) were screened out for better certainty[27,28] and encompassed in the present study.

The MOD13Q1 (TERRA) and MYD13Q1 (AQUA) products include NDVI and EVI, and quality assessment (QA) information for both was calculated from atmospherically corrected surface reflectance values and delivered as a 16-day composite image. NDVI is a nonlinear combination of red (R) and near-infrared (NIR) spectral radiances (eq. (1)), while EVI is optimized to enhance the vegetation signal through a decoupling of the canopy background signal (eq. (2)).

$$\mathrm{NDVI} = \frac{\rho_{\mathrm{NIR}} - \rho_{\mathrm{R}}}{\rho_{\mathrm{NIR}} + \rho_{\mathrm{R}}}, \tag{1}$$

$$\mathrm{EVI} = G\left[\frac{\rho_{\mathrm{NIR}} - \rho_{\mathrm{R}}}{\{\rho_{\mathrm{NIR}} + C_1(\rho_{\mathrm{R}}) - C_2(\rho_{\mathrm{B}}) + L\}}\right], \tag{2}$$

where ρ_{NIR}, ρ_{R} and ρ_{B} are the surface reflectance for the near-infrared, red and blue bands respectively; L the canopy background adjustment ($L = 1$); C_1 and C_2 coefficients of the aerosol resistance term that uses blue band of MODIS to correct for aerosol influences in the red band ($C_1 = 6$ and $C_2 = 7.5$), and G is a gain factor (= 2.5) (ref. 29).

For obtaining surface temperature over land region, MODIS eight-day composite LST products, i.e. MOD11A2 (TERRA) and MYD11A2 (AQUA) at 1 km spatial resolution were used. These LST products provide per-pixel temperature on the basis of emissivity values measured over thermal bands in a sequence of swath-based or grid-based global products.

For assessment of precipitation, Global Precipitation Measurement (GPM) Integrated Multi-Satellite Retrievals (IMERG) daily products were downloaded from the Goddard Earth Sciences Data and Information Services Center (GES DISC) website (https://disc.gsfc.nasa.gov). The IMERG products are available in the form of IMERG early (6 h latency), late (18 h latency) and final (3 months latency). Since GPM-IMERG final run data, which are most accurate and reliable[30] as they also incorporate monthly rain-gauge analysis into account was not available for study period, therefore adjusted precipitation for study period was calculated using eq. (3) and then precipitation anomaly was derived using eq. (4)

$$P_{\mathrm{A}} = P_{\mathrm{Ad}} - P_{\mathrm{F}}, \tag{3}$$

$$P_{\mathrm{Ad}} = P_{\mathrm{LL}} \times \frac{P_{\mathrm{F}}}{P_{\mathrm{L}}}, \tag{4}$$

where P_{A} is the anomaly of precipitation during the lockdown period, P_{Ad} the adjusted precipitation, P_{LL} the late run precipitation during the lockdown period, P_{F} the long-term mean of final run precipitation and P_{L} is the long-term mean of late run precipitation.

For soil moisture observations, the present study incorporates Advanced Microwave Scanning Radiometer 2 (AMSR-2) measured level-3 gridded dataset of soil moisture, which is retrieved at the 6.925 GHz channel using Land Parameter Retrieval Model (LPRM) at 10 km spatial resolution.

The MODIS data products were accessed from Land Processes Distributed Active Archive Center (LP DAAC) website (https://lpdaac.usgs.gov), while precipitation and soil moisture data were accessed from the GES DISC website.

The above-mentioned products were downloaded, preprocessed, clipped to the geographic extent of the study area and re-projected into the master map projection (i.e. UTM Zone 32N with WGS84 datum). Then the images were co-registered to the master image for accurate geographic comparisons and to reduce potential geometric errors. Further, the processed images were stacked to generate mean products for LST, NDVI, EVI and precipitation during the lockdown period and the long-term

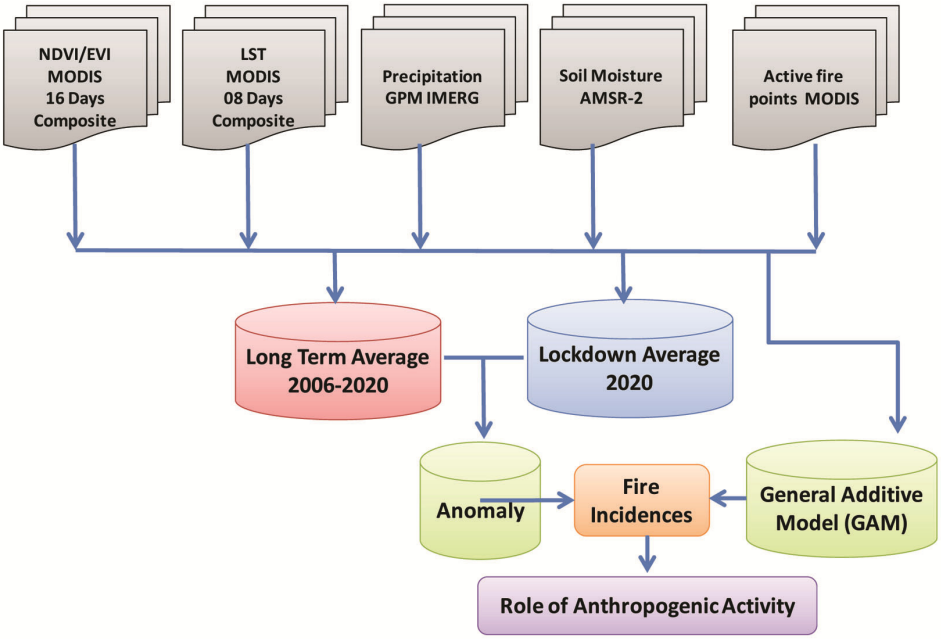

Figure 1. Schematic diagram of the data used and the workflow.

mean (2006–20) covering similar time period. Figure 1 is a schematic diagram of methodological workflow.

The generalized Additive Model (GAM) has been widely used in various aspects in environmental research[31]. It has substantially more flexibility because the relationships between independent and dependent variables are not assumed to be linear; rather smooth functions are applied to independent variables and then added to estimate the dependent variables. In the present study, GAM is used to assess the association of fire counts with EVI, NDVI, LST and precipitation. The entire dataset has been divided into two parts, since observation of the same parameters from TERRA and AQUA differs. First, association of fire counts with the four parameters was checked (eq. (5)), and then smoothening was applied, particularly to NDVI and EVI. Again the association was rechecked to determine if nonlinear smooth function could better resolve this association (eq. (6)).

$$g(E(F)) = \alpha + \mathrm{EVI} + \mathrm{NDVI} + \mathrm{LST} + P, \quad (5)$$

$$g(E(F)) = \alpha + s(\mathrm{EVI}) + s(\mathrm{NDVI}) + \mathrm{LST} + P, \quad (6)$$

where $(E(F))$ is the estimation of fire counts, α the intercept and s indicates the smooth function.

The various datasets on environmental parameters and active fire incidences in the Western Himalayan landscape show significant decrease in the forest fire incidences. The COVID-19 induced lockdown across the landscape of the Indian subcontinent has significantly reduced various factors like the aerosols and the other short-lived greenhouse gasses like NO_x, SO_2, etc. In New Delhi during the lockdown, the concentration of PM_{10} and $PM_{2.5}$ witnessed significant reduction of more than 50% compared to the pre-lockdown phase[32]. Studies have reported around 43%, 31%, 10% and 18% decreases in $PM_{2.5}$, PM_{10}, CO and NO_2 over major cities in India during the lockdown period compared to previous years[33]. Satellite-based observations and the literature have proved that the environmental and atmospheric pollution has considerably reduced due to the lockdown[34–36]. Observations from the Copernicus Sentinel-5P satellite showed that the average nitrogen dioxide concentration during the first lockdown phase when compared to the same time period in the previous was significantly lower by around 40–50% (https://www.esa.int).

Figure 2 shows the spatial occurrence of active fire points in study area during the last 15 years and illustrates that the southern slope of the Lower Himalaya and the Sivalik region in Uttarakhand have been mostly affected by such fires during this particular time period in the last 15 years; however, there is minimal trace of fires during the recent days of lockdown in 2020. Since most of the fire occurrences are attributed to anthropogenic activities, the lockdown period provides a window of opportunity to assess and understand fire incidences minus anthropogenic activities due to strict restrictions imposed during this period. We observed reduced anthropogenic footprints on the number of fire incidences across the Western Himalayan region, resulting in significant decrease in fire incidences across the landscape.

The number of active fire occurrences from MODIS during this temporal period was significantly high in the last 15 years (Figure 3 *a*). It was also observed that 73.3%

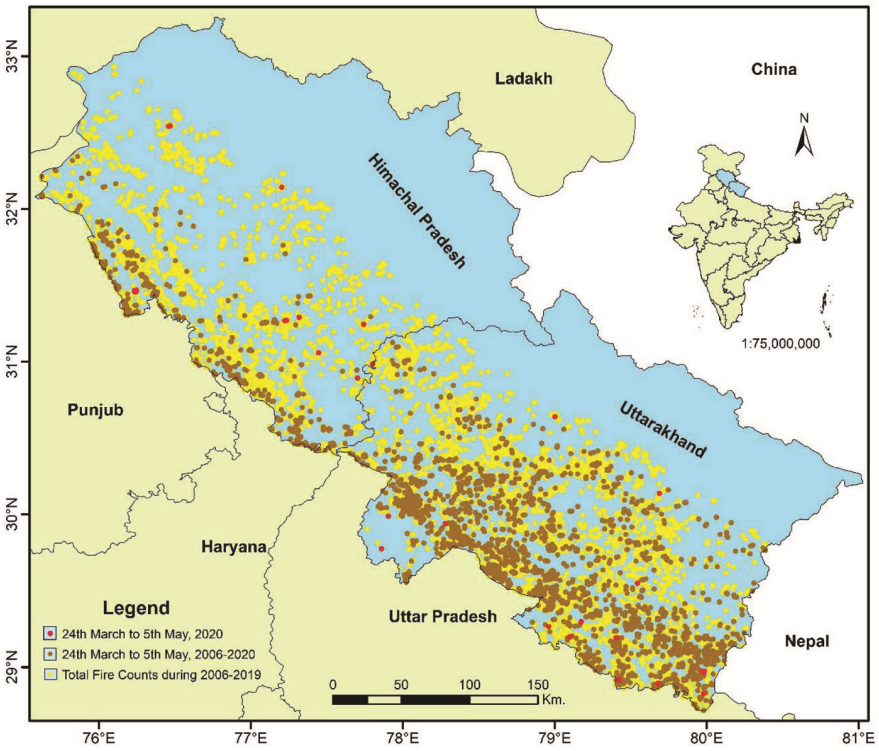

Figure 2. Cumulative fire occurrence during 24 March to 5 May 2020 and 2006–20 when compared with annual fire occurrence during 2006–20.

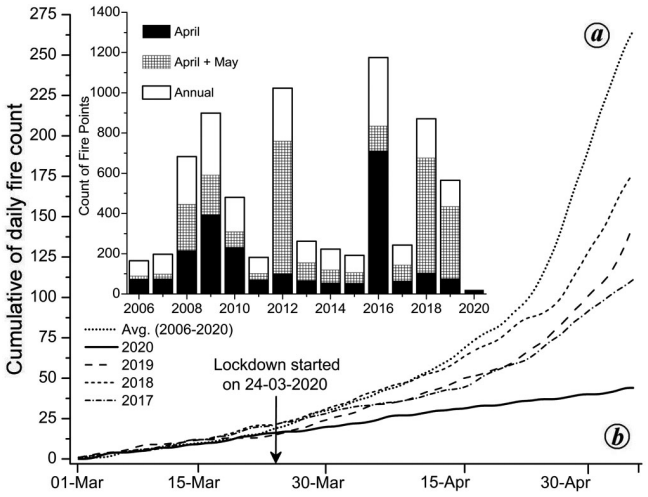

Figure 3. ***a***, Proportion of active fires in April and May during 2006–20. ***b***, Cumulative daily fire counts during 1 March to 5 May for an average of 2006–20, 2017, 2018, 2019 and 2020.

of annual fire in this region occurred during pre-monsoon season (March–May), of which 67.59% occurred only during April (30.2%) and May (37.39%); this indicates the peak period of fire season. Analysis showed that on average there were 164 fire incidences during this 43-day period of 2006–20. There were moderate to high extensive fire episodes, especially during 2008, 2009, 2010, 2012, 2018 and 2019 years, which alone increased the average to 294 fire incidences. Even if these extensive fire periods are excluded, non-severe fire years also have an average fire incidence occurrence rate of 60 during the 2006–20 time-frame. However, during 2020, the number of fire counts in this period was only 20, which is the lowest record for this time period in the last 15 years. Furthermore, the cumulative daily active fire points derived from MODIS show that the trajectory of the cumulative fire incidences from 24 March to 5 May is quite flat compared to those during the previous three years (2017–19), as well as the average cumulative observation for 2006–20 (Figure 3 *b*). The observations clearly point to the predominantly anthropogenic causes for fire initiation in the Western Himalayan landscape[4]. This may also be true for the rest of the Indian landscape and requires further studies.

The fire incidences have also been analysed in the context of precipitation, LST, NDVI, EVI and soil moisture. Figure 4 *a–c* highlights their interrelationship. It is interesting to note that during the period of lockdown, there has been high amounts of precipitation, which is significantly higher than the average in the last 15 years during the same period. However, the number of active fires is significantly lower than the years which had similar levels of precipitation (Figure 4 *c*). Though there has been an increase in precipitation, the spatial distribution shows greater increase towards the northwestern part of the

study area compared to the eastern part. The average cumulative precipitation during 2006–20 ranges between 75 and 125 mm, which is observed to increase to 175–250 mm during the current year in the same time period. On the contrary, if we compare the spatial pattern of soil moisture during the current lockdown period with the average soil moisture during the same phase for the previous eight years, not many significant changes are observed (Figure 5). The average soil moisture and that during the lockdown phase follow a similar pattern, indicating that higher precipitation during this year has not contributed to the build-up of moisture (Figure 4 *c*).

Under similar soil moisture regime, in the past fire count trajectory showed increase in fire counts from mid-March, unlike the current year where it has flattened. Spatial observations with reference to soil moisture show more or less similar pattern for the northwestern part of the study area, whereas towards the northeastern part there has been more significant decline in soil moisture during the study period in the current year than the average of the last eight years in the same time period. Furthermore, LST observations show a significant dip in 2020 across the landscape (Figure 4 *a* and *b*), which also corraborates the absence of forest fires in the region. The mean value of long-term averaged LST shows temperature ranges varying between 8.94°C and 16.08°C, which for the current lockdown phase has plummeted between 7.23°C and 13.57°C. LST, when observed spatially, has shown an overall decline of 0.73–3.15°C, majorly in the central and western parts of the study area (negative anomaly of 2.66–8.24°C) when compared to the northern and southern regions (Figure 6). LST has been used as an indicator of surface moisture status, consequences of land-cover changes on climate[37,38], and to study the association between maximum thermal anomalies, heat waves, melting ice sheets and droughts in tropical forests[39]. The NDVI- and EVI-based analysis indicates increase in values compared to the average values of previous 15 years, which are generally observed to be falling from mid-March and further in earlier time-frames (Figure 4 *a* and *b*). Spatial observations show that NDVI and EVI during this study period in 2020 compared to the average values of 2006–20 are significantly high over the northwestern part than towards the northeastern part, resulting in positive anomaly for both EVI (0.2–0.83) and NDVI (0.39–0.86) (Figure 6).

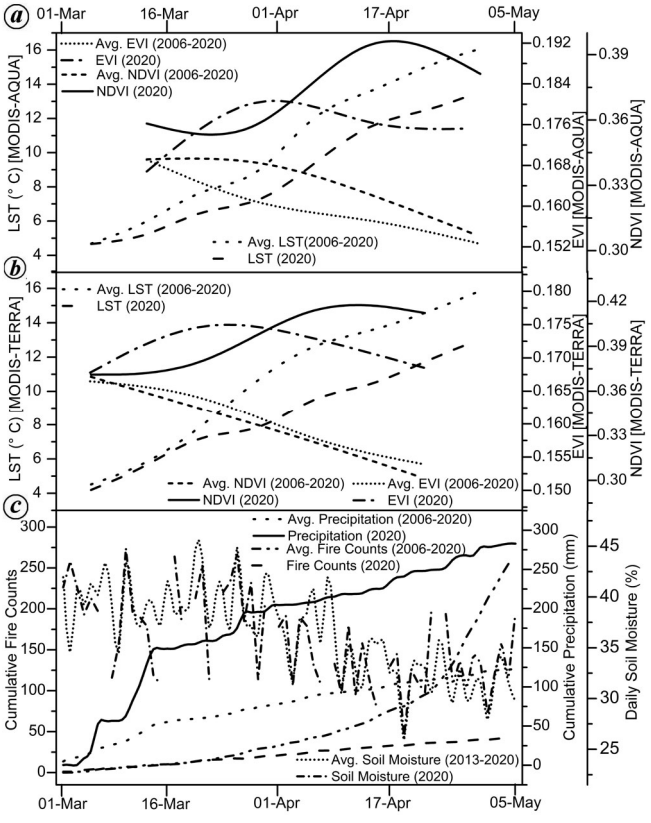

Figure 4. ***a***, ***b***, Temporal variation of normalized difference vegetation index (NDVI) and enhanced vegetation index (EVI) with land surface temperature (LST) during March and April 2020 and average of long-term period. ***c***, Temporal variation of soil moisture, precipitation and cumulative fire count during 1 March to 5 May 2020 and average of long-term period.

The analysis of various factors associated with forest fires in the Western Himalayan region points to the fact that there has been no reduction in the fuel load as indicated by the NDVI and EVI values. It is also observed that LST has increased consistently from 1 March to 5 May 2020, although this increase is comparatively less than the increase in LST during the previous three years as well as the average of 2006–20 (Figure 6). Figure 4 *c* indicates that even though precipitation has increased significantly, there is a consistent decrease in soil moisture and the trend is similar to the 15-year average. Hence, it can be safely concluded that moisture content in the litter has been adequate for fuel flammability in the region during recent days in 2020, like in the previous years. However, the decrease in daily fire counts and relatively flat cumulative fire progression point to the fact that due to less anthropogenic activities in the region, accidental fire incidences have reduced to a great extent. This is also corroborated by Figure 3 *b*, wherein the proportion of fire incidences during this time period of the last 14 years is significantly higher than that of 2020.

We have studied the association of fire incidences with several factors like precipitation, soil moisture, LST and vegetation indices to understand the above observations more rationally. Table 1 describes the performance of GAM in terms of R^2 and explained deviance. Initially, the model showed poor association for both dataset ($R^2 < 0.55$). After applying the smooth function to EVI and NDVI, R^2 value was greater than 0.75 and more than 80% deviance was explained in both the cases. Analysis showed that LST was the most significant parameter (0.01 significance level) and positively associated with fire occurrences. Precipitation was not significantly

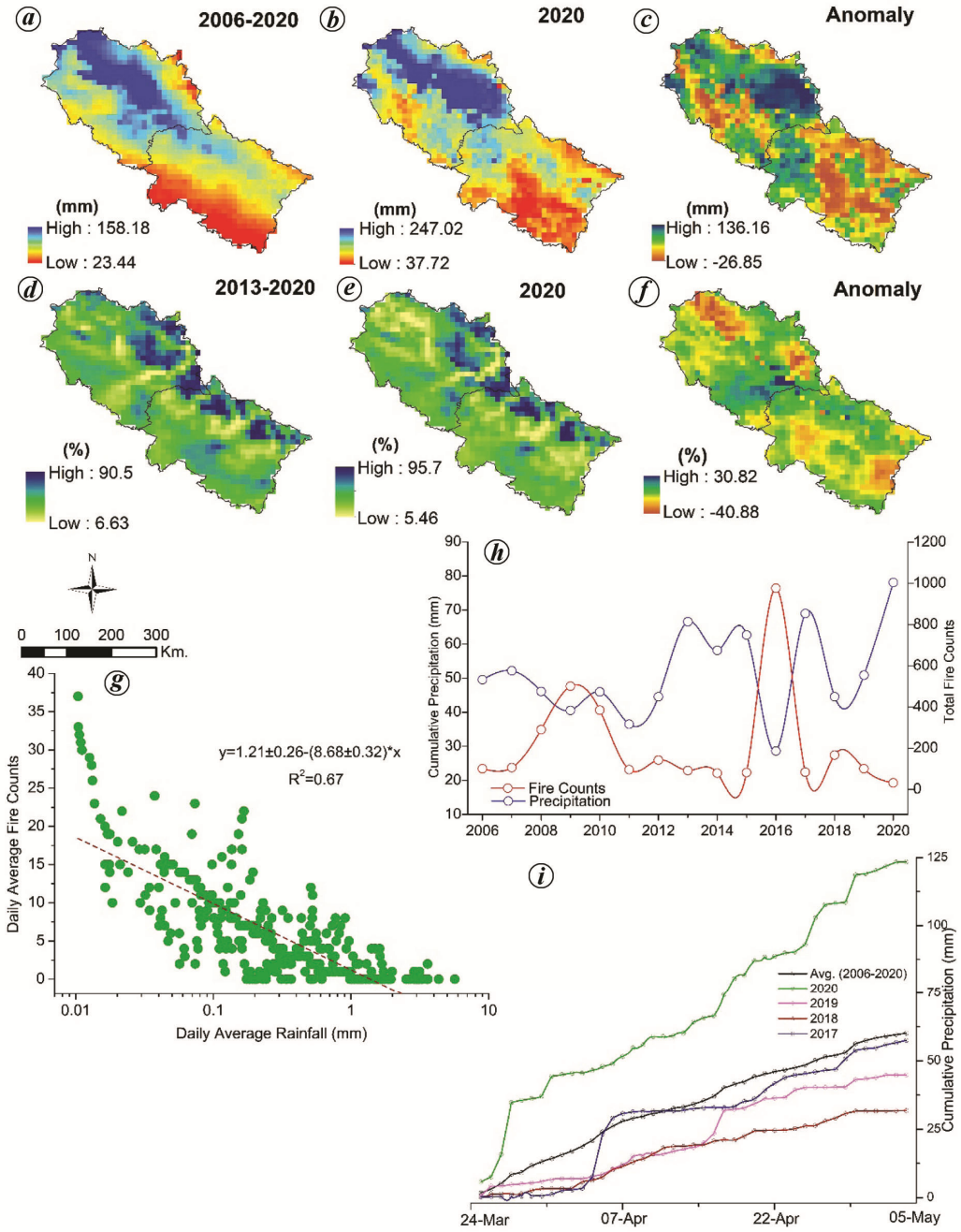

Figure 5. ***a***, Average precipitation during 24 March to 5 May (2006–2020); ***b***, Average precipitation during 24 March to 5 May (2020); ***c***, Precipitation anomaly between (***a***) and (***b***); ***d***, Average soil moisture during 24 March to 5 May (2013–2020); ***e***, Average soil moisture during 24 March to 5 May (2020); ***f***, Soil moisture anomaly between (***d***) and (***e***); ***g***, Regression plot of daily average fire count with daily average rainfall; ***h***, Yearly cumulative precipitation during 24 March to 5 May versus cumulative fire count during the same period; ***i***, Cumulative precipitation between 24 March to 5 May for average 2006–2020, 2020, 2019, 2018 and 2017.

related with fire; however, there was a negative association. Among vegetation indices, NDVI was found to be significantly associated at 0.01 significance level, whereas EVI was non-significant. This suggests that changes in NDVI and LST values are better indicators of variation in magnitude of fire incidences[40]. A study found that AQUA observations are more reliable than TERRA observations and that the association of vegetation indices with fire occurrence is profoundly nonlinear[41].

Taking into consideration all space-derived factors, during the current lockdown period precipitation was higher compared to the average for the last 15 years, but did not contribute to the build-up of soil moisture. Higher NDVI and EVI values in the lockdown phase unlike the average of previous years which shows declining trend, indicate that the lockdown has provided an opportunity for the canopy to sustain and have higher vigour; this was not visible earlier due to fire incidences. Improved

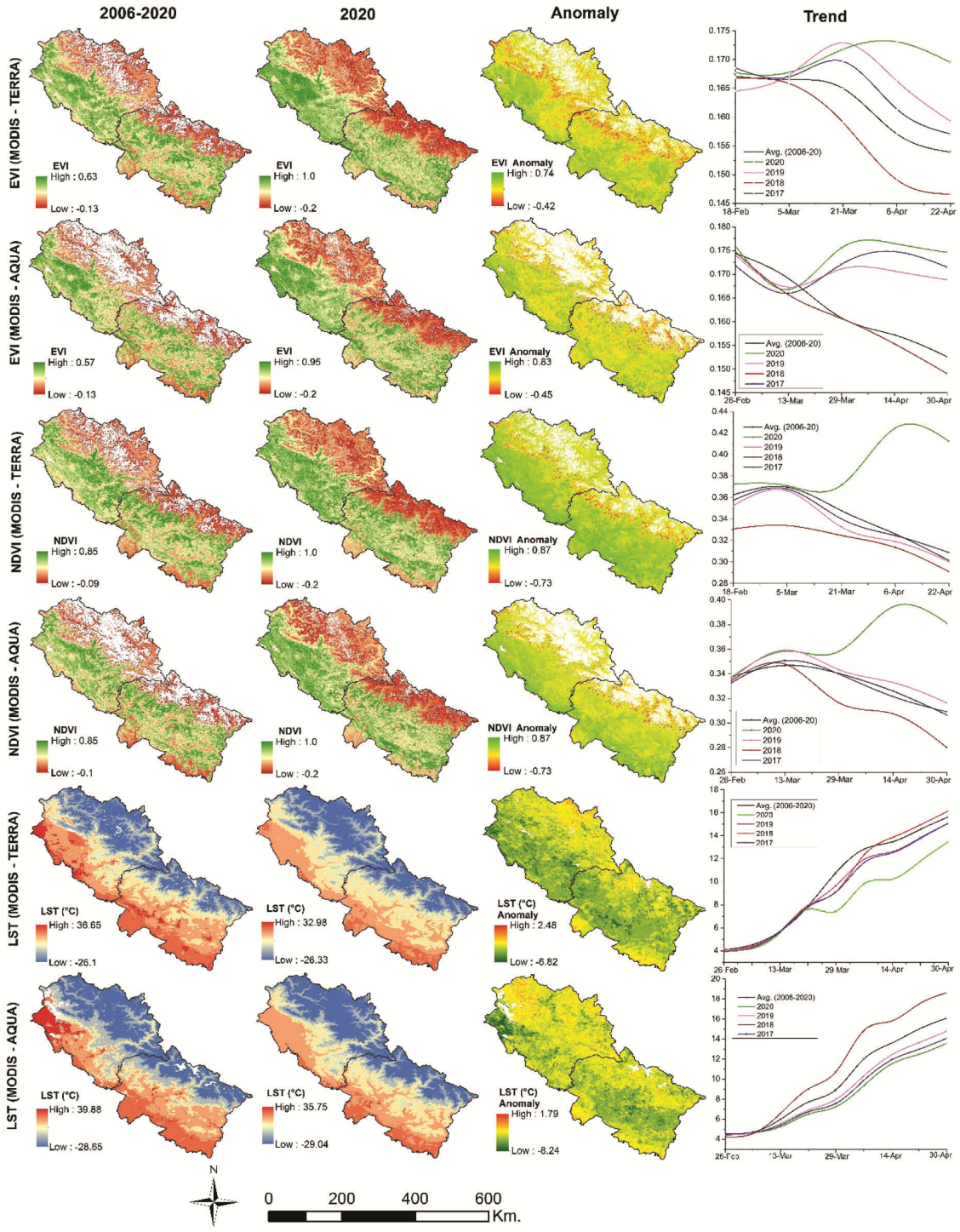

Figure 6. Variations in EVI, NDVI and LST during 24 March to 5 May 2006–20 and 2020 due to cessation of all anthropogenic activities in the Western Himalayan states of Uttarakhand and Himachal Pradesh, India.

canopy status and lesser fire incidences are also supported by the decline in LST. Further spatial layout of the above factors shows that the increase is higher in the western part of study area compared to the eastern part, but none of them witnessed higher fire incidence. These observations explain that though forest fuel is available in abundance, the triggering mechanism of forest fires (anthropogenic activities) is missing due to strict imposition of lockdown.

This study highlights the impact of anthropogenic activities, mainly the movement of people and vehicular traffic on fire incidences in the Western Himalayan landscape. Although rainfall during this period plays a significant role in the suppression of fire incidences in the

Table 1. Spatial statistical analysis of association between the environmental/meteorological parameters and forest fire occurrence

Parameters	MODIS-TERRA and precipitation		MODIS-AQUA and precipitation	
	Before smoothening	After smoothening	Before smoothening	After smoothening
R^2, Coefficient of determination	0.396	0.756	0.526	0.772
Deviance explained (%)	48	85.1	59.2	87.6
Intercept	310.52 ± 252.25	–606.8 ± 348.05	293.33 ± 190.58	–596.94 ± 241.3
Land surface temperature	78.39 ± 24.65**	52.85 ± 24.67*	40.76 ± 15.17*	47.49 ± 12.37**
Precipitation	–71.26 ± 48.77	–38.55 ± 28.4	–34.38 ± 29.77	–30.91 ± 27.35
Enhanced vegetation index	–1674.99 ± 1502.73	0.314^{+}	–3886.73 ± 3407.33	1.635^{+}
Normalized difference vegetation index	–4576.0 ± 2653.4	$5.779^{+,}$**	–4267.88 ± 1594.65*	$4.805^{+,}$**

^{+}F-value of smooth terms (EVI, NDVI). Significance level: *0.1, **0.01.

region, the dip in soil moisture content observed shows that the flammability of fuel load has not decreased significantly; however, fire incidences were significantly lower in April 2020. This coupled with high NDVI and EVI values could establish the fact that large-scale fire incidences which lead to degradation of the forests in this region are significantly less this year. This proves that the anthropogenic trigger is one of the most important factors for forest fire incidences in the region. This may have been the baseline fire scenario before economic liberalization and extensive infrastructure development associated with deforestation in the mountainous region of the western Himalaya. This scenario can also be used to estimate quantitatively the impact of various anthropogenic activities in fire incidences in the Indian landscape.

1. Collivignarelli, M. C., Abbà, A., Bertanza, G., Pedrazzani, R., Ricciardi, P. and Carnevale Miino, M., Lockdown for COVID-2019 in Milan: what are the effects on air quality? *Sci. Total Environ.*, 2020, **732**, 139280.
2. Yunus, A. P., Masago, Y. and Hijioka, Y., COVID-19 and surface water quality: improved lake water quality during the lockdown. *Sci. Total Environ.*, 2020, **731**, 139012.
3. Zambrano-Monserrate, M. A., Ruano, M. A. and Sanchez-Alcalde, L., Indirect effects of COVID-19 on the environment. *Sci. Total Environ.*, 2020, **728**, 138813.
4. Gupta, R. K., Impact of human influences on the vegetation of the Western Himalaya. *Vegetatio*, 1978, **37**, 111–118.
5. Bessie, W. C. and Johnson, E. A., The relative importance of fuels and weather on fire behavior in subalpine forests. *Ecology*, 1995, **76**, 747–762.
6. Tošić, I. *et al.*, Potential influence of meteorological variables on forest fire risk in Serbia during the period 2000–17. *Open Geosci.*, 2019, **11**, 414–425.
7. Reddy, C. S. *et al.*, Nationwide assessment of forest burnt area in India using Resourcesat-2 AWiFS data. *Curr. Sci.*, 2017, **112**(7), 1521–1532.
8. Albar, I., Jaya, I. N. S., Saharjo, B. H., Kuncahyo, B. and Vadrevu, K. P., Spatio-temporal analysis of land and forest fires in Indonesia using MODIS active fire dataset. In *Land-Atmospheric Research Applications in South and Southeast Asia* (eds Vadrevu, K. P., Ohara, T. and Justice, C.), Springer, Cham, Switzerland, 2018, pp. 105–127.
9. Jha, C. S. *et al.*, Monitoring of forest fires from Space – ISRO's initiative for near real-time monitoring of recent forest fires in Uttarakhand. *Curr. Sci.*, 2016, **110**, 2057–2060.
10. Vadrevu, K. P., Giglio, L. and Justice, C., Satellite based analysis of fire–carbon monoxide relationships from forest and agricultural residue burning (2003–11). *Atmos. Environ.*, 2013, **64**, 179–191.
11. Juárez-Orozco, S. M., Siebe, C. and Fernández y Fernández, D., Causes and effects of forest fires in tropical rainforests: a bibliometric approach. *Trop. Conserv. Sci.*, 2017, **10**, 19400829-1773720.
12. Ryan, K. C., Vegetation and wildland fire: implications of global climate change. *Environ. Int.*, 1991, **17**, 169–178.
13. Chowdhury, E. H. and Hassan, Q. K., Use of remote sensing-derived variables in developing a forest fire danger forecasting system. *Nat. Hazards*, 2013, **67**, 321–334.
14. Chen, F., Niu, S., Tong, X., Zhao, J., Sun, Y. and He, T., The impact of precipitation regimes on forest fires in Yunnan Province, Southwest China. *Sci. World J.*, 2014, 1–9.
15. Holden, Z. A. *et al.*, Decreasing fire season precipitation increased recent western US forest wildfire activity. *Proc. Natl. Acad. Sci., USA*, 2018, **115**, E8349–E8357.
16. Lafon, C. W. and Quiring, S. M., Relationships of fire and precipitation regimes in temperate forests of the eastern United States. *Earth Interact.*, 2012, **16**, 1–15.
17. Bartsch, A., Balzter, H. and George, C., The influence of regional surface soil moisture anomalies on forest fires in Siberia observed from satellites. *Environ. Res. Lett.*, 2009, **4**, 045021.
18. Chaparro, D., Vall-llossera, M., Piles, M., Camps, A. and Rudiger, C., Low soil moisture and high temperatures as indicators for forest fire occurrence and extent across the Iberian Peninsula. In IEEE International Geoscience and Remote Sensing Symposium (IGARSS), Milan, Italy, 2015, pp. 3325–3328.
19. Chauhan, J. S., Gautam, A. S. and Negi, R. S., Natural and anthropogenic impacts on forest structure: a case study of Uttarakhand state. *Open Ecol. J.*, 2018, **11**, 38–46.
20. Suresh Babu, Roy, A. and Prasad, P. R., Forest fire risk modeling in Uttarakhand Himalaya using TERRA satellite datasets. *Eur. J. Remote Sensing*, 2016, **49**, 381–395; doi:10.5721/EuJRS20164921.
21. Saha, S., Anthropogenic fire regime in a deciduous forest of central India. *Curr. Sci.*, 2002, **82**, 1144–1147.
22. Semwal, R. L. and Mehta, J. P., Ecology of forest fires in chir pine (*Pinus roxburghii* Sarg.) forests of Garhwal Himalaya. *Curr. Sci.*, 1996, **70**, 426–427.
23. Singh, R. D., Gumber, S., Tewari, P. and Singh, S. P., Nature of forest fires in Uttarakhand: frequency, size and seasonal patterns in relation to pre-monsoonal environment. *Curr. Sci.*, 2016, **111**, 398.
24. Champion, H. G. and Seth, S. K., *A Revised Survey of the Forest Types of India*, Manager of Publications, Government of India, Delhi, 1968.
25. Giglio, L., Schroeder, W. and Justice, C. O., The collection 6 MODIS active fire detection algorithm and fire products. *Remote Sensing Environ.*, 2016, **178**, 31–41.
26. Giglio, L., Descloitres, J., Justice, C. O. and Kaufman, Y. J., An enhanced contextual fire detection algorithm for MODIS. *Remote Sensing Environ.*, 2003, **87**, 273–282.

27. Sabani, W., Rahmadewi, D. P., Rahmi, K. I. N., Priyatna, M. and Kurniawan, E., Utilization of MODIS data to analyze the forest/land fires frequency and distribution (case study : Central Kalimantan Province). *IOP Conf. Ser.: Earth Environ. Sci.*, 2019, **243**, 012032.
28. Tanpipat, V., Honda, K. and Nuchaiya, P., MODIS hotspot validation over Thailand. *Remote Sensing*, 2009, **1**, 1043–1054.
29. Huete, A. R., Liu, H. Q., Batchily, K. and van Leeuwen, W., A comparison of vegetation indices over a global set of TM images for EOS-MODIS. *Remote Sensing Environ.*, 1997, **59**, 440–451.
30. Huffman, G. J., Bolvin, D. T., Braithwaite, D., Hsu, K., Joyce, R., Xie, P. and Yoo, S. H., NASA global precipitation measurement (GPM) integrated multi-satellite retrievals for GPM (IMERG). Algorithm Theoretical Basis Document (ATBD) Version, 2015, 4, p. 26.
31. Hastie, T. and Tibshirani, R., Generalized additive models. *Stat. Sci.*, 1986, **1**, 297–318.
32. Mahato, S., Pal, S. and Ghosh, K. G., Effect of lockdown amid COVID-19 pandemic on air quality of the megacity Delhi, India. *Sci. Total Environ.*, 2020, **730**, 139086.
33. Sharma, S., Zhang, M., Anshika, Gao, J., Zhang, H. and Kota, S. H., Effect of restricted emissions during COVID-19 on air quality in India. *Sci. Total Environ.*, 2020, **728**, 138878.
34. Dantas, G., Siciliano, B., França, B. B., da Silva, C. M. and Arbilla, G., The impact of COVID-19 partial lockdown on the air quality of the city of Rio de Janeiro, Brazil. *Sci. Total Environ.*, 2020, **729**, 139085.
35. Kerimray, A. *et al.*, Assessing air quality changes in large cities during COVID-19 lockdowns: the impacts of traffic-free urban conditions in Almaty, Kazakhstan. *Sci. Total Environ.*, 2020, **730**, 139179.
36. Nakada, L. Y. K. and Urban, R. C., COVID-19 pandemic: impacts on the air quality during the partial lockdown in São Paulo state, Brazil. *Sci. Total Environ.*, 2020, **730**, 139087.
37. Nemani, R. R., Pierce, L. E. and Running, S. W., Developing satellite-derived estimates of surface moisture status. *J. Appl. Meteor.*, 1993, **32**(3), 548–557.
38. Li, L., Zhang, L., Xia, J., Gippel, C. J., Wang, R. and Zeng, S., Implications of modelled climate and land cover changes on runoff in the middle route of the south to north water transfer project in China. *Water Resour. Manage.*, 2015, **29**, 2563–2579.
39. Mildrexler, D. J., Zhao, M., Cohen, W. B., Running, S. W., Song, X. P. and Jones, M. O., Thermal anomalies detect critical global land surface changes. *J. Appl. Meteorol. Climatol.*, 2018, **57**, 391–411.
40. Vlassova, L., Pérez-Cabello, F., Mimbrero, M. R., Llovería, R. M. and García-Martín, A., Analysis of the relationship between land surface temperature and wildfire severity in a series of Landsat images. *Remote Sensing*, 2014, **6**, 6136–6162.
41. Giglio, L., Characterization of the tropical diurnal fire cycle using VIRS and MODIS observations. *Remote Sensing Environ.*, 2007, **108**(4), 407–421.

ACKNOWLEDGEMENTS. We thank the Chairman, Indian Space Research Organisation, Department of Space, Government of India for support. We also thank FIRMS for active fire points, LP DAAC for spatial data of NDVI, EVI and LST and GES DISC for precipitation and soil moisture data.

Received 13 May 2020; revised accepted 19 May 2020

doi: 10.18520/cs/v119/i2/390-398

Foliar micromorphometric adaptations of micropropagated plants of *Oldenlandia herbacea* (L.) Roxb. – an important medicinal herb

J. Revathi[1], M. Manokari[2], S. Priyadharshini[1] and Mahipal S. Shekhawat[1,*]

[1]Biotechnology Laboratory, Kanchi Mamunivar Government Institute for Postgraduate Studies and Research, Puducherry 605 008, India
[2]Siddha Clinical Research Unit, Central Council for Research in Siddha, Palayamkottai, Tirunelveli 727 002, India

An effective *in vitro* regeneration protocol is essential to improve the natural population of conservation-prioritized plants species. The micropropagation techniques are considered cost-effective if the survival chance of tissue-cultured plants is excellent in field conditions. Comparative foliar micromorphometric characteristics were analysed in this study, to determine the sequential developmental adaptations of foliages of *Oldenlandia herbacea* plantlets under *in vitro* and field conditions. The leaf constants showed considerable variations in stomatal morphology, type and density (decreased from 60.0 to 40.75), vein islet density (increased from 8.3 to 13.5) and raphides density (increased from 20.9 to 36.0) in the foliage of tissue-cultured and field-transferred plantlets. The micromorphometric changes reflect the developmental improvements taking place in the greenhouse and field transplantation of *O. herbacea* plants, which are essential for the survival of plantlets under natural conditions.

Keywords: Foliar micromorphology, *in vitro* regeneration, medicinal herb, micropropagation, *Oldenlandia herbacea*.

OLDENLANDIA herbacea (L.) Roxb. (family Rubiaceae), commonly known as chayaparpatika, is considered as the most important medicinal plant for its febrifuge, anthelmintic, expectorant, stomachic and anti-inflammatory properties[1]. It is a seasonal plant which completes its life cycle in 3–4 months. Conventionally, this plant is propagated only by seeds. The plants are being uprooted by the traditional drug practitioners before seed-setting; therefore, the population of *Oldenlandia* species has depleted sharply in recent years[2].

In vitro regeneration techniques offer valuable prospects in large-scale production of medicinal plants using bare minimum starting materials from the donor plant[3]. This also reduces the impact of over-exploitation on the native population of medicinal plants. However, the extensive use of *in vitro* technology is constrained due to difficulties in the survivorship of micropropagated plantlets under natural conditions after transplantation[4].

*For correspondence. (e-mail: smahipal3@gmail.com)